

Supporting Information

Combination of Density Functional Theory and Microkinetic Study to the Mn-Doped CeO₂ Catalysts for CO Oxidation: A Case Study to Understand the Doping Metal Content

Weiyu Song,^{†,§} Lulu Chen,^{†,§} Jianlin Deng,[†] Meizan Jing,[†] Huiling Zheng,[†] Jian Liu,^{*,†} and Zhen Zhao^{†,‡}

[†]State Key Laboratory of Heavy Oil Processing, College of Science, China University of Petroleum-Beijing, Beijing 102249, China

[‡]Institute of Catalysis for Energy and Environment, Shenyang Normal University, Shenyang 110034, China

[§]W.S. and L.C. authors contribute equally to this paper.

* Corresponding author.

E-mail: liujian@cup.edu.cn

Table S1. The oxygen vacancy formation energies and CO adsorption energies on $\text{MnCe}_{x-1}\text{O}_{2x}(111)$ surface with different k-point.

	k-point	$E_{\text{O},v}$	Energy difference/eV	$E_{\text{CO,ads}}$	Energy difference/eV
$\text{MnCe}_{x-1}\text{O}_{2x}(111)$	$1 \times 1 \times 1$	0.08	0	-0.28	0
	$2 \times 2 \times 1$	0.1	0.02	-0.28	0
	$2 \times 2 \times 1$	0.1	0.02	-0.27	0.01
	$4 \times 4 \times 1$	0.14	0.06	-0.28	0

Table S2. The oxygen vacancy formation energies and CO adsorption energies on different surface with different size of supercell.

model	$E_{\text{O},v}/\text{eV}$	Energy difference/eV	$E_{\text{CO,ads}}/\text{eV}$	Energy difference /eV
$\text{MnCe}_{x-1}\text{O}_{2x}(111)$ (4×4)	0.05		-0.29	
$\text{MnCe}_{x-1}\text{O}_{2x}(111)$ (3×3)	0.08	0.03	-0.28	0.01
$\text{Mn}_2\text{Ce}_{x-2}\text{O}_{2x}(111)$ (4×4)	0.01		-0.29	
$\text{Mn}_2\text{Ce}_{x-2}\text{O}_{2x}(111)$ (3×3)	-0.01	0.02	-0.28	0.01
$\text{Mn}_3\text{Ce}_{x-3}\text{O}_{2x}(111)$ (4×4)	0.77		-0.27	
$\text{Mn}_3\text{Ce}_{x-3}\text{O}_{2x}(111)$ (3×3)	0.73	0.04	-0.32	0.05

Table S3. The oxygen vacancy formation energies and CO adsorption energies on $\text{MnCe}_{x-1}\text{O}_{2x}(111)$ surface with different layers.

	layers	$E_{\text{O},v}/\text{eV}$	Energy difference/eV	$E_{\text{CO,ads}}/\text{eV}$	Energy difference/eV
$\text{MnCe}_{x-1}\text{O}_{2x}(111)$	3	0.08	0	-0.28	0
	4	0.10	0.02	-0.30	0.02
	5	0.19	0.11	-0.34	0.06

Table S4. The relative energies, the spin magnetic moments and the oxidation state of Mn atoms in double Mn doped ceria (111)

Position		Relative energy/eV	The spin magnetic moments of Mn atoms/ μB	The oxidation state of Mn atoms
surface	a	0	3.887, 3.916	+3; +3
	1NN b	0.47	3.870, 4.019	+3; +3
	c	1.77	3.866, 3.808	+3; +3
	d	1.82	3.881, 3.986	+3; +3
	2NN e	2.24	3.888, 3.885	+3; +3
	f	2.06	3.886, 4.018	+3; +3
	3NN g	2.06	3.885, 3.872	+3; +3
	1NN a	1.28	3.883; 3.958	+3, +3
subsurface	b	1.74	3.214; 3.934	+4; +3
	2NN c	0.81	3.879; 3.931	+3; +3
	d	2.39	3.874; 3.956	+3; +3
	3NN e	1.44	3.881; 3.953	+3; +3
	f	2.37	3.879; 3.954	+3; +3
	g	2.31	3.878; 3.949	+3; +3
	4NN h	2.39	3.877; 3.955	+3; +3

Table S5. The relative energies, the spin magnetic moments and the oxidation state of Mn atoms in treble Mn doped ceria (111)

Position		Relative energy/eV	The spin magnetic moments of Mn atoms/ μB	The oxidation state of Mn atoms
surface	a	0	3.906; 3.875; 3.959	+3; +3; +3
	1NN b	0.77	3.888; 3.808; 3.903	+3; +3; +3
	c	1.30	3.892; 3.813; 4.118	+3; +3; +3
	d	0.95	3.884; 3.791; 3.895	+3; +3; +3
	e	0.75	3.888; 3.886; 4.003	+3; +3; +3
	3NN f	1.19	3.888; 3.907; 3.927	+3; +3; +3
	1NN a	0.99	3.896; 3.791; 3.934	+3; +3; +3
	b	1.36	3.864; 3.728; 4.130	+3; +3; +3
subsurface	2NN c	0.71	3.883; 3.839; 3.927	+3; +3; +3
	d	1.59	3.887; 3.808; 4.326	+3; +3; +3
	3NN e	1.43	3.883; 3.795; 4.181	+3; +3; +3
	f	1.64	3.889; 3.836; 4.247	+3; +3; +3
	g	1.34	3.887; 3.807; 3.947	+3; +3; +3
	4NN h	1.42	3.884; 3.876; 3.947	+3; +3; +3

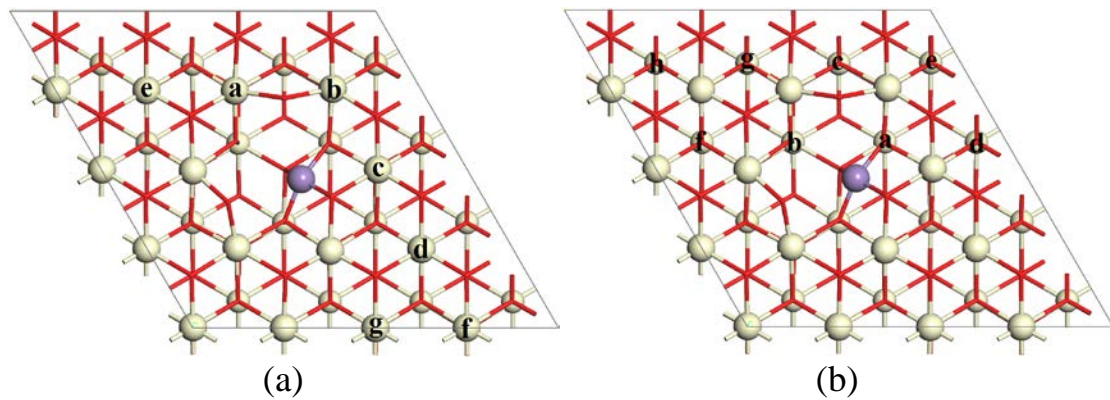


Figure S1. The possible sites for substitutions of the second Mn atom. (a), the possible sites in the surface; (b), the possible sites in the subsurface.

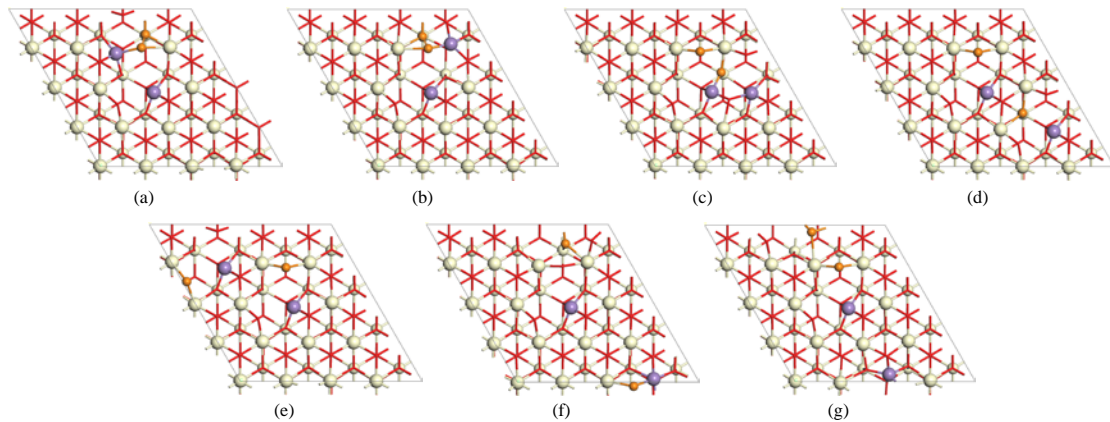


Figure S2. The detailed optimized configurations of double Mn atoms doped ceria (111) surface. The second Mn replaces Ce in the surface. Except that the oxygen atom in which charge transfer occurs is marked with an orange ball, the remaining oxygen atoms are represented by lines.

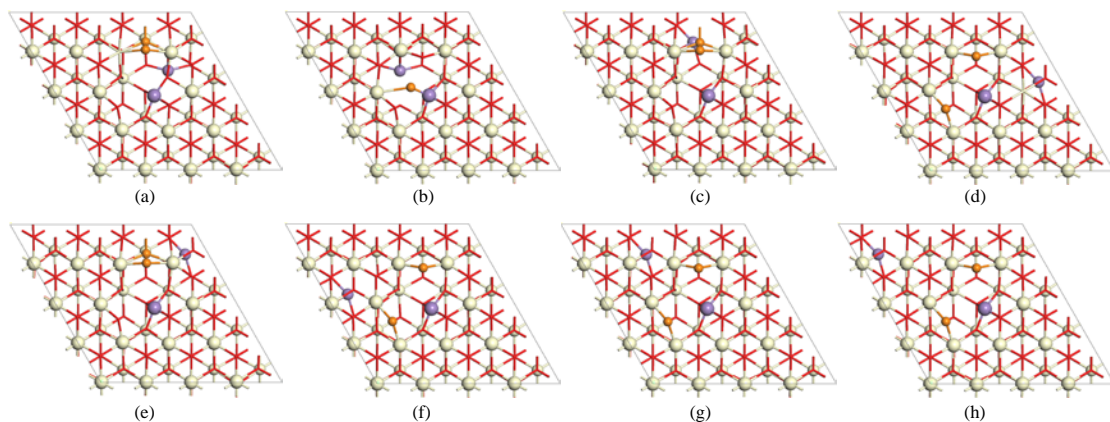


Figure S3. The detailed optimized configurations of double Mn atoms doped ceria (111) surface. The second Mn replaces Ce in the subsurface.

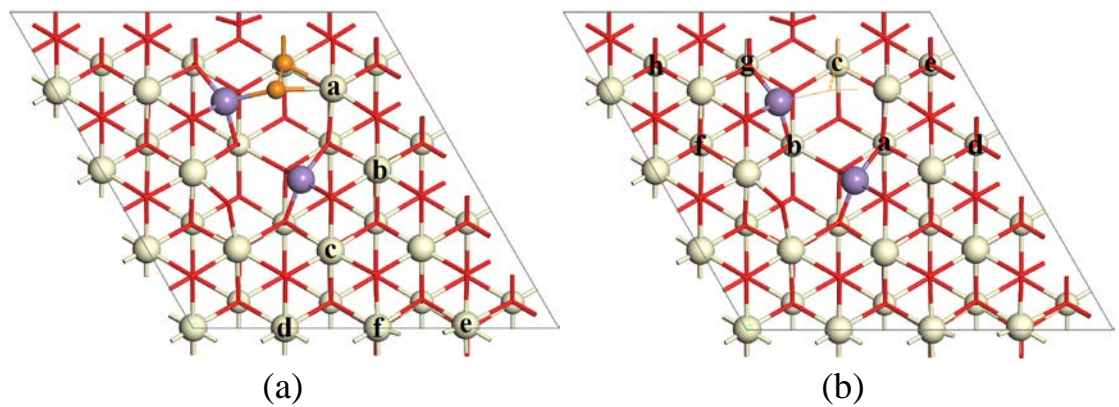


Figure S4. The possible sites for substitutions of the third Mn atom. (a), the possible sites in the surface; (b), the possible sites in the subsurface. In order to facilitate the marking of the Ce surface of the subsurface, we use orange lines to represent O_2^{2-} species in (b).

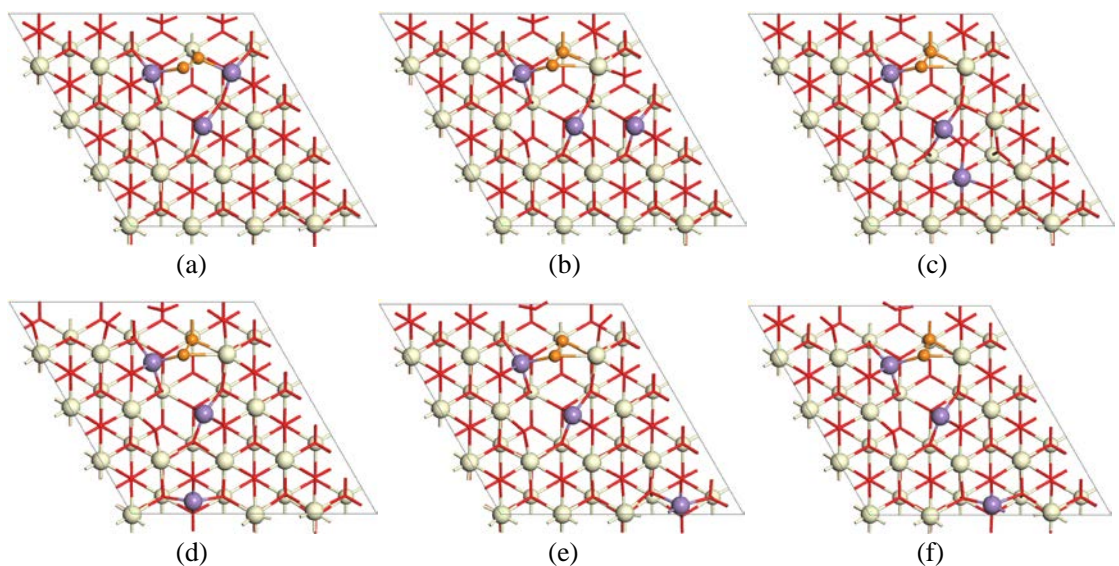


Figure S5. The detailed optimized configurations of treble Mn atoms doped ceria (111) surface.
The third Mn replaces Ce in the surface.

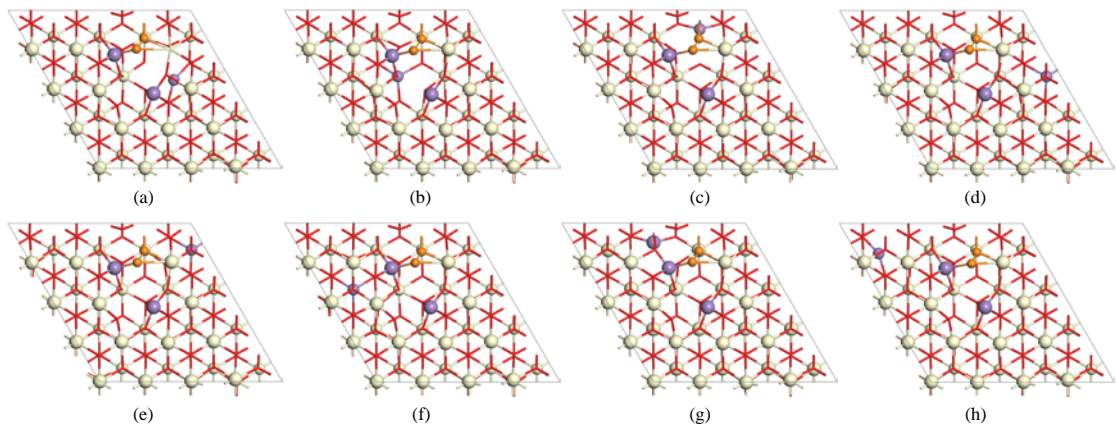


Figure S6. The detailed optimized configurations of triple Mn atoms doped ceria (111) surface.
The third Mn replaces Ce in the subsurface.

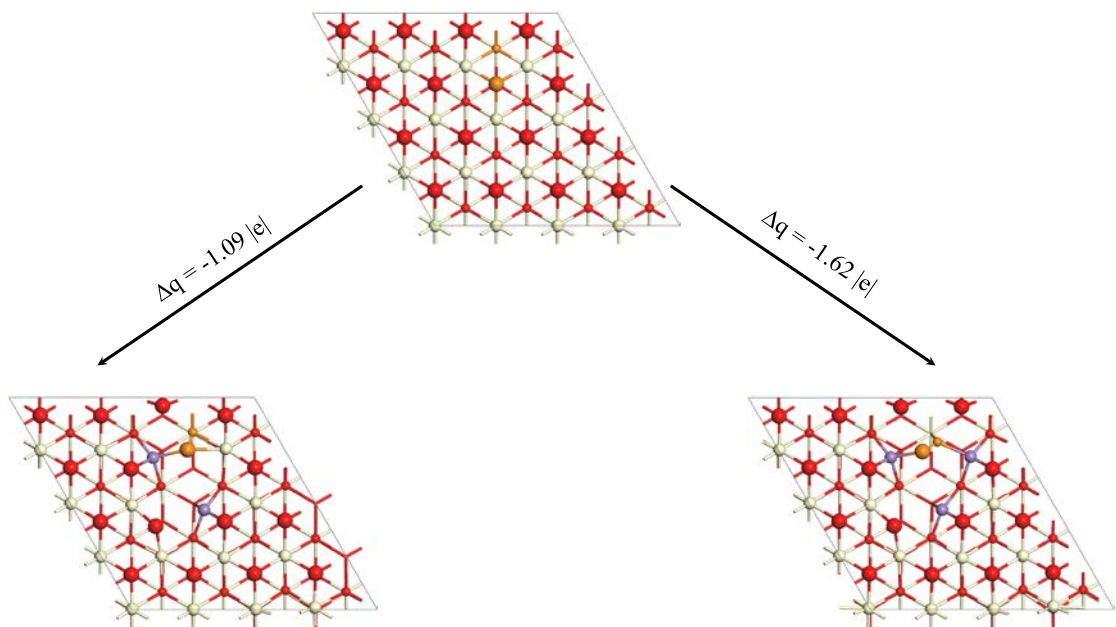


Figure S7. Bader charge difference of $\text{CeO}_2(111)$ surface, $\text{Mn}_2\text{Ce}_{x-2}\text{O}_{2x}(111)$ surface and $\text{Mn}_3\text{Ce}_{x-3}\text{O}_{2x}(111)$ surface.